

Analysis of the mass balance time series of glaciers in the Italian Alps

L. Carturan^{*1,6}, C. Baroni^{2,3,6}, M. Brunetti⁴, A. Carton^{5,6}, G. Dalla Fontana^{1,6}, M. C. Salvatore^{2,6}, T. Zanoner^{5,6,7},
G. Zuecco¹

¹ Dipartimento Territorio e Sistemi Agro-Forestali, University of Padova, Viale dell'Università 16, 35020, Legnaro, Padova, Italy

² Dipartimento di Scienze della Terra, University of Pisa, Via S. Maria 53, 56126, Pisa, Italy

³ IGG-CNR, Via Giuseppe Moruzzi 1, 56124, Pisa, Italy

⁴ ISAC-CNR, Via Gobetti 101, 40129, Bologna, Italy

⁵ Dipartimento di Geoscienze, University of Padova, Via Gradenigo 6, 35131, Padova, Italy

⁶ Comitato Glaciologico Italiano, Corso Massimo d'Azeglio 42, 10125, Torino, Italy

⁷ CNR-IRPI, Strada delle Cacce 73, 10135, Torino, Italy

Corresponding author: luca.carturan@unipd.it

Abstract

This work presents an analysis of the mass balance series of nine Italian glaciers, which were selected based on the length, continuity and reliability of observations. All glaciers experienced mass loss in the observation period, which is variable for the different glaciers and ranges between 10 and 47 years. The longest series display increasing mass loss rates, which were mainly due to increased ablation during longer and warmer ablation seasons. The mean annual mass balance (B_a) in the decade from 2004 to 2013 ranged from -1788 mm to -763 mm w.e. y^{-1} . Low-altitude glaciers with low elevation ranges are more out of balance than the higher, larger and steeper glaciers, which maintain residual accumulation areas in their upper reaches. The response of glaciers is mainly controlled by the combination of Oct-May precipitations and Jun-Sep temperatures, but rapid geometric adjustments and atmospheric changes lead to modifications in their response to climatic variations. In particular, a decreasing correlation of B_a with the Jun-Sep temperatures and an increasing correlation with Oct-May precipitations are observed for some glaciers. In addition, the Oct-May temperatures tend to become significantly correlated with B_a , possibly indicating a decrease in the fraction of solid precipitation, and/or increased ablation, during the accumulation season. Because most of the monitored glaciers have no more accumulation area, their observations series are at risk due to their impending extinction, thus requiring a soon replacement.

35

36 **1 Introduction**

37 The mass balance of glaciers is a key variable for monitoring strategies of the Earth climate system because
38 it is the direct and undelayed response of glaciers to atmospheric conditions. Other reactions of glaciers to
39 climatic changes, such as the fluctuations of the front, are more easy and immediate to measure but
40 represent indirect, delayed and filtered signals (WGMS, 2008; Zemp et al., 2005).

41 The direct glaciological method (Østrem and Brugman, 1991) is the standardized method in worldwide
42 glacier monitoring strategies. This method consists of in-situ measurements of the surface accumulation
43 and ablation, taken at single points and then extrapolated and integrated to yield the glacier-wide surface
44 mass balance (Kaser et al., 2003; Cogley et al., 2011). The World Glacier Monitoring Service (WGMS)
45 collects and publishes mass balance data of glaciers obtained by the glaciological method as part of global
46 climate-related observation systems (Zemp et al., 2009; WGMS, 2012 and 2013, and earlier issues).

47 The European Alps are one of the regions of the world with the highest density of glaciers that are subject
48 to mass balance observations. Twenty five glaciers have ongoing and continuous mass balance series with
49 at least 10 years of observations, and 11 of them are longer than 30 years
50 (<http://www.wgms.ch/metadatabrowser.html>, last access: 27 September 2015). In the Italian Alps, nine
51 glaciers have ongoing and continuous mass balance series longer than 10 years, and only one glacier (the
52 Careser Glacier) has a series longer than 30 years.

53 The mass balance series of the glaciers in the Italian Alps have not yet been reviewed and analysed jointly.
54 The Italian glaciers may have a peculiar behaviour compared to the glaciers from other regions of the
55 European Alps, because of the differences in glacier characteristics, climatic features and trends of
56 meteorological variables (Brunetti et al., 2006 and 2009; Auer et al., 2007). Differences may occur in the
57 response of the glaciers in different sub-regions of the Italian Alps or with different characteristics, which
58 have not been recognized. It is also interesting to highlight possible feedbacks in the response of Italian
59 glaciers to atmospheric changes.

60 Therefore, this work aims to i) analyse and compare the direct mass balance series of the glaciers in the
61 Italian Alps, ii) understand the behaviour of the measured glaciers in relation to the observed climatic
62 trends, and iii) highlight possible future requirements for the mass balance monitoring strategy in the
63 Italian Alps.

64

65 **2 Available mass balance series**

66 In this work, we analyse the glaciers with at least 10 years of continuous and ongoing mass balance
67 measurements, which were obtained using the direct glaciological methods and published in peer reviewed
68 journals or in the WGMS publications (CGI, 1914–1977 and 1978–2011; Baroni et al., 2012, 2013, 2014;
69 WGMS, 2012 and 2013, and earlier issues). "Continuous" indicates the series with data gaps <10%,
70 and "ongoing" indicates that the mass balance observations have been performed in the last two years (i.e.,
71 the 2012 and 2013 hydrological years). These criteria ensure the comparability of the series, a sufficient
72 length in the temporal analyses and reliability of the measurements and calculations.

73 Nine monitored glaciers fulfil these characteristics in the Italian Alps and are clustered in three geographic
74 areas (Fig. 1). The two monitored glaciers in the Gran Paradiso Group (Western Alps), i.e., Grand Etrèt
75 (since 2002) and Ciardoney (since 1992), are rather small (area < 1 km²) and have low mean elevations and
76 low elevation ranges (Table 1). Snowfall is the prevailing feeding source, but windborne snow and
77 avalanching also contribute to snow accumulation.

78 The longest series of mass balance measurements in the Italian Alps has been collected on the Careser
79 Glacier, in the Ortles-Cevedale (Eastern Alps, Fig. 1) since 1967. Currently, this glacier is undergoing rapid
80 shrinking and fragmentation in smaller units. It is characterized by a flat surface, prevailing southern
81 exposure, quite low mean elevation and feeding by snowfall. Its area decreased from 5 km² in 1967 to 1.6
82 km² in 2012 (Carturan et al., 2013a). In the 1980s, observations started in two other glaciers of the Ortles-
83 Cevedale: Fontana Bianca and Sforzellina. These two small mountain glaciers (area <0.5 km²) have different
84 characteristics: Fontana Bianca is rather steep with negligible debris cover and mainly fed by snowfall,
85 whereas Sforzellina is flatter, debris-covered in its lower part and fed by avalanches in its upper part. In the
86 2000s, mass balance observations began in the Lunga Glacier and in the southern branch of La Mare Glacier,
87 which are larger valley glaciers (1.9 and 2.2 km², respectively) that reach higher elevations (3378 and 3518
88 m, respectively) and mainly fed by snowfall.

89 In Val Ridanna (Breonie Occidentali Group, Eastern Alps, Fig. 1), the measurements began in 1996 in the
90 Pendente Glacier and were extended to the Malavalle Glacier in 2002. The first glacier is a 0.9 km² wide
91 mountain glacier, characterized by a flat surface, low mean elevation, southern exposure and significant
92 accumulation from windborne snow. The second glacier is a much larger (6.9 km²) valley glacier with higher
93 mean and maximum elevation and mainly fed by snowfall.

94

95 **3 Methods**

96

97 **3.1 Mass balance measurements and calculations**

98 Point measurements of the annual mass balance in the ablation area consist of repeated readings of
99 ablation stakes, which are made of aluminium, wood or plastic and drilled into the ice/firn using hand drills
100 or steam drills. In the accumulation area, the depth of the snow at the end of the ablation season is
101 measured using hand probes, and its density is determined in snowpits. Snow depth soundings and density
102 measurements in the snowpits or by hand coring devices are also used for winter mass balance
103 measurements, which are performed on all glaciers except Sforzellina. The summer mass balance is derived
104 by subtracting the winter mass balance from the annual mass balance. The density of measuring points
105 varies among different glaciers in relation to their extent, accessibility and complexity of the mass balance
106 distribution (Fig. 2). The ablation stake density ranges from 4 points km⁻² (Malavalle Glacier) to 45 points
107 km⁻² (Sforzellina Glacier). The density of snow depth soundings for the winter mass balance determination
108 ranges from 15 points km⁻² (Malavalle Glacier) to 142 points km⁻² (Fontana Bianca Glacier).

109 Point measurements are interpolated and extrapolated to the entire area of the glaciers using different
110 procedures. In the Grand Etrèt and Ciardoney glaciers, each ablation stake is assumed representative of a
111 specific part of the glacier, where the mass balance distribution is assumed homogeneous. Then, a
112 weighted mean is calculated, using the area of the homogeneous parts into which the glacier is subdivided

113 as weights (<http://www.pngp.it/>, last access: 27 September 2015; <http://www.nimbus.it/>, last access: 27
114 September 2015). In Malavalle and Pendente glaciers, the area is divided into “sub-catchments”, and for
115 each sub-catchment, a linear regression of point balances vs. altitude is calculated and used for the
116 spatialization (<http://www.provinz.bz.it/wetter/glacierreport.asp>, last access: 27 September 2015). In
117 Careser Glacier, the even distribution of the mass balance and good coverage of measurement points
118 enable the use of automatic interpolation algorithms (Spatial Analyst Tools) in the ESRI-ArcGIS software.
119 Manual drawing of balance isolines is used for the remaining Sforzellina, Fontana Bianca, La Mare and
120 Lunga glaciers (Catasta and Smiraglia, 1993; Cannone et al., 2008;
121 <http://www.provinz.bz.it/wetter/glacierreport.asp>; Carturan, 2016). The measurements are performed
122 close to the time of maximum and minimum mass balance during the year, when the glacier and
123 atmospheric conditions are favourable for field surveys. The “floating-date” time measurement system is
124 used for all glaciers (Cogley et al., 2011).

125 Typical random errors reported in the literature for glacier-wide mass balance estimates obtained with
126 these methods are of about ± 200 mm w.e. γ^{-1} (Lliboutry, 1974; Braithwaite and Olesen, 1989; Cogley and
127 Adams, 1998; Cogley, 2009). The accuracy indicated by the investigators carrying out mass balance
128 measurements in the nine Italian glaciers range between ± 0.05 and 0.30 m w.e. γ^{-1} (WGMS, 2015; Carturan,
129 2016). Assessments based on the comparison between the direct and the geodetic mass balance have been
130 published for the Careser, La Mare and Lunga glaciers, indicating that the discrepancy between the two
131 methods is lower than the lowest detectable bias (following Zemp and others, 2013), and revealing that a
132 calibration of the direct mass balance results is not required (Carturan et al., 2013a; Galos et al., 2015;
133 Carturan, 2016).

134

135 **3.2 Meteorological series**

136 The climatic variables used in this work consist of synthetic records of the monthly mean temperature and
137 total monthly precipitation, which are obtained for the centre of the three main geographic areas described
138 in Sect. 2, using the procedure reported in Brunetti et al. (2012). Starting from sparse meteorological data
139 recorded at meteorological stations, the synthetic meteorological series are generated using the anomaly
140 method (New et al., 2000; Mitchell and Jones, 2005). This method is based on the assumption that the
141 spatio-temporal structure of the signal of a meteorological variable over a given area can be described by
142 the superimposition of two fields: the climatological normals over a given reference period (i.e., the
143 climatologies) and the departures from them (i.e., the anomalies). The climatologies are linked to the
144 geographic features of the territory and characterized by remarkable spatial gradients; the departures are
145 linked to the climate variability and change, and they are generally characterized by higher spatial
146 coherence.

147 Under this assumption, the climatologies and anomalies can be reconstructed in completely independent
148 manners and based on different data sets. For climatologies, the priority is the high spatial resolution, and a
149 short time span (few decades) is sufficient. A lower spatial resolution is sufficient for the anomalies, but
150 more importance is given to the data quality and availability of long records. Thus, all series that were used
151 for the anomaly component were subjected to homogenization.

152 The interpolation methods are different for the two components. The climatologies, which are
153 characterized by high spatial gradients, were reconstructed using the procedure in Brunetti et al. (2014),
154 exploiting the relationship between the meteorological variable and the physical characteristics of the

155 terrain. The anomalies, which are characterized by higher spatial coherence, were reconstructed using
156 weighted averages as described in Brunetti et al. (2006). The weights are horizontal and vertical distance
157 weighting functions, with the addition of an angular weight that accounts for the anisotropy in the
158 distribution of stations around the sites. Finally, the two fields were superimposed to obtain the temporal
159 series in absolute values for each site.

160

161 **3.3 Analyses of the mass balance and meteorological series**

162 The time series of annual mass balance (B_a), winter mass balance (B_w), summer mass balance (B_s) and
163 Accumulation Area Ratio (AAR, i.e., the ratio of the area of the accumulation zone to the area of the glacier)
164 were analysed and compared to highlight the possible trends, break points, common behaviour and
165 peculiarities of single glaciers and/or single years. To highlight the systematic differences among the
166 glaciers, the mean values of B_a , B_w , B_s and AAR were calculated in the common period of observation from
167 2004 to 2013. The decadal means of B_a for the Italian glaciers were compared to the decadal means for a
168 sample of nine representative glaciers of the European Alps (Zemp et al., 2005). The correlations among the
169 B_a series of different glaciers and among B_a of single glaciers with the respective series of B_w and B_s were
170 subsequently computed, to identify possible groups of glaciers with similar behaviours and to understand
171 the relative importance of the seasonal components of mass balance.

172 Linear trends and moving averages were calculated for the time series of air temperature and precipitation
173 to highlight the climatic drivers of the observed glacier changes. In particular, we focused on the
174 precipitation of the accumulation season, from October to May (Oct-May), and on the air temperature of
175 the ablation season, from June to September (Jun-Sep) (Pelto, 2008; Carturan et al., 2013b), computing
176 their correlation with B_a and performing multiple linear regression analyses. For the four glaciers with the
177 longest mass balance series (Careser, Fontana Bianca, Sforzellina and Ciardoney), we performed a moving
178 correlation analysis of B_a vs. the seasonal and annual temperature and precipitation, to recognize possible
179 changes and/or trends in their response and sensitivity to climatic fluctuations, e.g., ascribable to
180 geometric adjustments. A correlation analysis of B_w , B_s and B_a versus the seasonal (December to February
181 and October to May) and annual mean North Atlantic Oscillation (NAO) index was performed, using the
182 mass balance data of glaciers from Italy and from other nations of the European Alps. Five-year (i.e.,
183 current +/- 2 years) triangular moving averages have been applied to the time series before correlation
184 analyses, to highlight possible convergent low-frequency patterns which are not detectable at the annual
185 scale.

186

187 **4 Results and discussion**

188 **4.1 Analysis of mass balance series**

189 **Annual balance**

190 The longest available series for the glaciers in the Italian Alps clearly show a trend towards more negative
191 B_a in the observation period (Fig. 3), and one or two change points, which were identified using the
192 'Changepoint' R package (Killick and Eckley, 2014). In particular, the series of Careser Glacier shows three
193 phases: i) the period from 1967 to 1980 with near equilibrium conditions (mean $B_a = -132$ mm w.e. y^{-1} , STD
194 = 540 mm w.e.); ii) the period from 1981 to 2002 with imbalanced conditions (mean $B_a = -1192$ mm w.e. y^{-1} ,

195 STD = 517 mm w.e.); and iii) the period after 2002 with stronger imbalance (mean $B_a = -1926$ mm w.e. y^{-1} ,
196 STD = 725 mm w.e.). The transition of 2002-03 is also observable for the Fontana Bianca, Sforzellina and
197 Pendente glaciers, whose measurements started in the 1980s and 1990s. Their mean B_a values changed
198 from -599, -868 and -703 mm w.e. y^{-1} , before 2002, to -1257, -1471 and -1308 mm w.e. y^{-1} after 2002,
199 respectively. This transition is less obvious for the Ciardoney Glacier, which experienced a notably negative
200 mass balance already in 1998 and 1999.

201 **Seasonal balance and AAR**

202 The B_w and B_s series have some gaps but suggest that the increased mass loss rates were mainly ascribable
203 to increased ablation (and associated positive feedbacks) instead of decreased snow accumulation. These
204 results are consistent with previous works, which indicate that the mass changes of the glaciers in the Alps,
205 at the annual and decadal scale, are mainly driven by the summer balance (e.g., Schonert et al., 2000;
206 Vincent et al., 2004; Zemp et al., 2008; Huss et al., 2015).

207 The AAR series show that the accumulation area almost vanished from all glaciers in the 2000s except the
208 years 2001, 2010 and 2013, when several glaciers were close to balanced-budget conditions mainly as a
209 result of the increased B_w . In these years, the highest increase in AAR occurred in the Fontana Bianca
210 Glacier, which is steep and exposed to the east. On the contrary, the AAR did not significantly increase in
211 the neighbouring Careser Glacier, which is flatter and mainly exposed to the south (Table 1). This behaviour
212 is uncommon for flat glaciers because they should be more sensitive to variations of the Equilibrium Line
213 Altitude (ELA) than the steeper glaciers (Benn and Evans, 2010), and reveals that the Careser Glacier is
214 almost completely below the current ELA, also in the years of ELA minima. La Mare and Malavalle glaciers,
215 which are larger and cover a wider elevation range (Table 1), show more persistent accumulation areas,
216 although their size is too small to ensure balanced-budget conditions.

217 The B_a and B_s values of different glaciers tend to diverge in years with largely negative mass balance and
218 converge in years closer to equilibrium (1993, 2001, 2010 and 2013, Fig. 3). Reinforcing processes and
219 feedbacks likely amplify the differences among the glaciers in imbalanced years, particularly the decrease in
220 the glacier-average albedo caused by the early disappearance of snow from low-lying, flat and less
221 topographic-shielded glaciers, and by the accumulation of dust and debris on the surface. B_w also shows the
222 alternation of years with small/large variability among the glaciers, but this behaviour cannot be clearly
223 related to the magnitude of the snow accumulation, as observed in the two high-accumulation years 2009
224 (high variability) and 2013 (low variability). In this case, the spatial variability of the precipitation during the
225 accumulation season, which is larger than the spatial variability of air temperature in the ablation season,
226 determines the interannual variability of B_w for single glaciers, which is further controlled by snow
227 redistribution processes. Snow redistribution appears more effective for the Pendente, Grand Etrèt and
228 Ciardoney glaciers, leading to over-accumulation in snow-rich winters (e.g., in 2009) and larger interannual
229 variability of B_w . Correlation coefficients calculated between B_w and October-May precipitations range
230 between 0.73 and 0.78 are significant at the 0.05 level only for Careser, La Mare, Lunga, Fontana Bianca
231 and Malavalle, while they are not statistically significant for Pendente, Grand Etrèt and Ciardoney, in line
232 with the hypothesised higher importance of snow redistribution processes in these three glaciers.

233

234 **Comparisons in the common period from 2004 to 2013 and spatial representativeness**

235 In the period from 2004 to 2013, significantly higher B_w is observed for Pendente and Grand Etrèt,
236 compared with the other glaciers in the same geographic area (Table 2), explaining the persistence of these
237 two ice bodies at such low altitude (Table 1). In the same period, the Careser Glacier had the lowest
238 average B_a and AAR, whereas the Malavalle and La Mare glaciers had the highest average B_a , B_s and AAR,
239 retaining accumulation areas in their upper parts. However, the mean AARs were remarkably low for all
240 analysed glaciers, and far from balanced-budget conditions ($AAR_0 = 0.55 - 0.58$, Dyurgerov et al., 2009;
241 Mernild et al., 2013). Overall, low-altitude and flat glaciers with low elevation ranges are more out of
242 balance than the steeper glaciers at higher altitude with higher elevation ranges, as acknowledged in
243 various other studies (e.g., Furbish and Andrews, 1984; Benn and Evans, 2010; Carturan et al., 2013b;
244 Fischer et al., 2015).

245 At the regional scale, the spatial representativeness of five Italian mass balance glaciers can be assessed on
246 the basis of the geodetic mass balance calculations performed by Carturan et al., (2013b). In the period
247 from the 1980s to the 2000s, the average geodetic mass balance rate of the 112 glaciers in the Ortles-
248 Cevedale Group has been -0.69 m w.e. y^{-1} . If we consider the average geodetic mass balance in the same
249 period as an index of the spatial representativeness for single glaciers, we obtain in decreasing order: i) La
250 Mare with -0.64 m w.e. y^{-1} , ii) Sforzellina with -0.86 m w.e. y^{-1} , iii) Fontana Bianca with -0.90 m w.e. y^{-1} , iv)
251 Lunga with -1.00 m w.e. y^{-1} , and v) Careser with -1.43 m w.e. y^{-1} . These results confirm that a proper
252 assessment of the spatial representativeness is required when inferring regional-scale mass balance
253 estimates using single glaciers. Geodetic calculations only exist for few areas in the Italian Alps (e.g., Galos
254 et al., 2015) and do not include the other four mass balance glaciers analysed in this study. Therefore it was
255 not possible to evaluate their spatial representativeness at the regional scale. Similarly, quantitative
256 assessments of the representativeness of all the nine glaciers at the scale of the entire Italian Alps will
257 require further investigations, integrating in-situ measurements, remotely sensed observations and
258 numerical modelling (WGMS, 2015).

259 **Comparison with other glaciers in the European Alps**

260 The response of Italian glaciers to the climatic conditions of the last decades is similar to that of nine
261 representative glaciers of the entire European Alps (Zemp et al., 2005; Fig. 4), although single glaciers
262 display different mass loss rates (Table 2). The Italian glaciers display ~ 200 - 250 mm w.e. y^{-1} more negative
263 B_a until 2002 and ~ 200 mm w.e. y^{-1} less negative B_a since then. Therefore, it can be assessed that the mean
264 B_a values for the Italian and “European” glaciers are fairly similar. Comparable results were obtained by
265 Huss et al., (2015), who compared the decadal mean B_a of glaciers from France, Switzerland, Austria and
266 Italy. These comparisons may be affected by the loss of spatial representativeness of some glaciers (e.g.
267 Careser in the Italian Alps and Sarennes in the French Alps) and by the different subsets of Italian glaciers
268 which are useable in the four different sub-periods. In the last decade, the inclusion of La Mare and
269 Malavalle glaciers in the Italian subset and the concurrent sharp decrease of B_a for the Sarennes, St. Sorlin
270 and Gries glaciers explain the different behaviours of the two groups of glaciers. However, the smaller
271 Italian glaciers (average area = 1.79 km²) may have a shorter response time to climatic changes, adjusting
272 their geometry faster than the larger glaciers (average area = 3.63 km²) which are representative of the
273 European Alps (Hoelzle et al., 2003; Abermann et al., 2009). The rapid shrinking and fragmentation of
274 Careser Glacier is a good example: in the last decade, its area has halved, and it completely lost the parts
275 subject to higher ablation (Carturan et al., 2013a). Changes in the general atmospheric circulation and
276 spatial distribution of precipitation could also have played a role and will be discussed in Sect. 4.2.

277 **Correlation analyses**

278 There is a generally high correlation among the B_a values of the analysed glaciers (Table 3). The series of
279 Careser, Fontana Bianca and La Mare glaciers show a highly significant correlation with most other glaciers,
280 even if they have different characteristics or are far away. On the contrary, the Lunga Glacier shows a lower
281 correlation and lower statistical significance with the glaciers of the same mountain group. However, it has
282 the shortest series, and most importantly, it does not include the highly negative B_a of 2003, which certainly
283 increases the correlation among other glaciers. There are notably high correlations in the Ortles Cevedale
284 between Careser and La Mare and between Fontana Bianca and La Mare glaciers. A similarly high
285 correlation is observed between Pendente and Malavalle glaciers in Val Ridanna, whereas there is a much
286 lower correlation between the two glaciers of the Gran Paradiso Group, which suggests that differences in
287 local topo-climatic factors can be decisive on such small ice bodies (e.g., Kuhn, 1995; DeBeer and Sharp,
288 2009; Carturan et al., 2013c; Scotti et al., 2014; Colucci and Guglielmin, 2015).

289 For most glaciers, B_a is more correlated to B_s than to B_w (Table 4), which further confirms the importance of
290 summer ablation. The relevance of the snow redistribution and over-accumulation on the Pendente and
291 Grand Etrèt glaciers is indicated by the higher correlation of their B_a with B_w . On La Mare Glacier, the two
292 seasonal components have similar correlations with B_a . However, these results are influenced by the length
293 of the observation period and the presence/absence of extreme years with high accumulation (e.g., 2001)
294 or high ablation (e.g., 2003) in the observation series of individual glaciers. For the analysed glaciers, no
295 significant correlation was found between B_s and B_w .

296

297 **4.2 Climatic controls**

298 In the period from 1961 to 2013, there are highly significant warming trends for the Jun-Sep air
299 temperature (Fig. 5a, b and c); they are highest in the Gran Paradiso Group ($0.40^\circ\text{C decade}^{-1}$) and lowest in
300 Val Ridanna ($0.35^\circ\text{C decade}^{-1}$). The three phases in the longer B_a and B_s series of glaciers (Fig. 3) can be
301 recognized as periods with stationary Jun-Sep temperature, separated by switches in the early 1980s and
302 after the peak of 2003. The warming trends are lower in the accumulation season and range from 0.25 to
303 $0.27^\circ\text{C decade}^{-1}$ (Fig. 5d, e and f), but thermal inversions at the valley weather stations could have partially
304 masked the warming at the altitude of the glaciers in this season. The transition towards higher Oct-May
305 temperature occurred in the late 1980s, after a minimum in the first half of the same decade. A distinct
306 warm peak in Oct-May temperature occurred in 2007. The warming trend led to increased duration of the
307 ablation period. The number of days per year with maximum temperature exceeding 0°C , extrapolated at
308 3000 m a.s.l. from the series of the Careser diga weather station (2600 m a.s.l. in the Ortles-Cevedale Group)
309 with a lapse rate of $0.65^\circ\text{C}/100\text{ m}$, increased from 160-170 in the 1960s-1970s to about 190 in the late
310 1990s and 2000s (Fig. 6).

311 The precipitation does not show any significant trend in the accumulation season (Fig. 7d, e and f). The
312 moving averages display oscillations of 10-20% above and below the 1961-1990 mean, which lasted
313 approximately 10-15 years and were higher in the Gran Paradiso Group than in the Ortles-Cevedale and Val
314 Ridanna. Periods with below-average precipitation are recognized in the 1960s, first half of 1970s, and
315 1990s, whereas periods with above-average precipitation occurred in the second half of 1970s and the first
316 half of 1980s. The last 10-15 years were characterized by precipitation close to the mean, with important
317 maxima in 2001, 2009 and 2013, and minima in 2007 and 2012. Similarly to the findings from Durand et al.,
318 (2009a and b) and Eckert et al., (2011) for the French and western Swiss Alps, change points in winter
319 precipitation of Ortles-Cevedale and Val Ridanna series were identified in 1977, corresponding to an

320 increase of about 10-12%. This finding is remarkable because, until present, this change point has been
321 identified to have a rather regional significance limited to the western Alps. Linear trends of summer
322 precipitation are positive but not statistically significant. The interannual variability of the Jun-Sep
323 precipitation is remarkably higher in the Gran Paradiso Group (Fig. 7a, b and c).

324 Large scale circulation patterns, such as the North Atlantic Oscillation (NAO) and the Northern Hemisphere
325 blocking frequency, are connected with the temporal and spatial variability of winter precipitation in the
326 Alps (Quadrelli et al., 2001). Several studies highlighted contrasting behaviour of precipitation anomalies in
327 the Oct-May period between the northern and southern Alps, i.e. opposite correlation with indexed large
328 scale circulation patterns (e.g., Quadrelli et al., 2001; Schmidli et al., 2002, Brunetti et al., 2006) and
329 opposite long-term trends in the seasonal precipitation totals (e.g., Brunetti et al., 2006 and 2009; Auer et
330 al., 2007). This characteristic, and the tendency towards a decreasing NAO index in the last two decades
331 (<http://www.cpc.ncep.noaa.gov/products/precip/CWlink/pna/new.nao.shtml>, last access: 11 February
332 2016; Fig. 8), leading to increased winter precipitation in the southern side of the Alps, may provide an
333 additional explanation for the different behaviour of “European” and “Italian” glaciers shown in Fig. 4.
334 Opposite effects of the NAO on the winter precipitation and glacier mass balance in the northern and
335 southern parts of the Eastern Alps were also reported, for example, by Marzeion and Nesje (2012).

336 Our correlation analysis confirm that prevailing negative correlation exists between the B_w of Italian glaciers
337 and the NAO in the accumulation season, whereas positive correlations prevail in other nations (Table 5),
338 with the exception of Gries Glacier which however is close to the Italian border. The winter precipitation
339 anomalies of the three geographic areas where the Italian mass balance glaciers are located (Section 2) are
340 also anti-correlated with the winter NAO (Spearman correlation significant at the 0.01 level). In line with
341 the findings of Reichert et al., (2001), Six et al., (2001), and Thibert et al., (2013), a negative correlation was
342 calculated between B_s/B_a and the NAO in the accumulation season. For the Italian glaciers the albedo
343 feedback from wet/dry winters (with low/high NAO, respectively) can at least partly explain this behaviour.
344 For glaciers in other countries however, given the prevailing positive correlation of their B_w with the winter
345 NAO, the link between B_s/B_a and the winter NAO is not so obvious and deserves additional analyses.

346 The examination of meteorological series confirms that increased ablation and the related feedbacks are
347 the main causes of the increased imbalance of the analysed Italian glaciers, as observed in Sect. 4.1. This
348 result is further corroborated by the higher correlation of B_a with the Jun-Sep temperature than with the
349 Oct-May precipitation, at least for the glaciers with longer observation series (Careser, Fontana Bianca,
350 Sforzellina and Ciardoney, Table 6). B_a of glaciers with shorter observation series is not significantly
351 correlated with the Jun-Sep temperature; instead, two of them (La Mare and Lunga) show a correlation
352 with the Oct-May precipitation. Combining the Oct-May precipitation and Jun-Sep temperature in a
353 multiple linear regression model leads to highly significant coefficients for both variables, even when the
354 single seasonal components are not correlated with B_a (e.g., for the Pendente and La Mare glaciers).
355 Approximately two-thirds of the B_a variance can be explained by the multiple linear regression. The
356 poorest results were obtained for the two glaciers in Val Ridanna (Pendente and Malavalle) and the Grand
357 Etrèt Glacier. As the first two glaciers are close to the main Alpine divide, they likely benefit from the high
358 orographic uplift that locally enhances precipitation (Schwarb, 2000), but which cannot be accounted for by
359 the multiple regression model due to the lack of weather stations in that area. In addition, the multiple
360 regression model does not account for accumulation by windborne snow on the Pendente and Grand Etrèt
361 glaciers.

362 The Careser, Fontana Bianca and Pendente glaciers display significant negative correlations between their
363 B_a and the Oct-May temperature. For the Careser Glacier, there is also a negative correlation between B_w
364 and the Oct-May temperature. Normally, in this period, most precipitation falls as snow, and the glaciers
365 have negligible ablation and low temperature sensitivity (Oerlemans and Reichert, 2000). However,
366 increasing temperature starts to lead to significant ablation in this period and to reduce the fraction of solid
367 precipitation as clearly detectable in the ablation season (Carturan et al., 2013b). An emblematic example is
368 the warm accumulation season of 2006-07, when the liquid precipitation reached 3000-3100 m a.s.l. (24
369 October 2006), and ice ablation exceeded 50 cm at 3000 m a.s.l. on the Careser and La Mare glaciers.

370 The correlation between B_a of Careser Glacier and the Oct-May temperature starts to become significant in
371 the late 1980s, as shown in the moving correlation analyses (30-year time window in Fig. 9). In the first 20
372 years, the correlation was absent or not statistically significant. These results are consistent with the
373 discussed effects of increasing temperature on the ablation and partitioning between liquid and solid
374 precipitation (Beniston et al., 2003). Reducing the window size from 30 to 15 years leads to a noisier signal
375 and in this case the correlation between B_a and Oct-May temperature does not reach the 95% significance
376 thresholds. However, it is interesting to remark the reversal of the correlation sign from positive in the first
377 years to negative in the last years.

378 The four glaciers in Fig. 9 (Careser, Fontana Bianca, Sforzellina and Ciardoney) share a common trend
379 towards i) a non-significant moving correlation between B_a and the Jun-Sep temperature and ii) a
380 significant moving correlation between B_a and Oct-May precipitation. This behaviour is probably related to
381 the snow-rich accumulation seasons of 2001, 2009 and 2013, and to the fact that the ablation season is
382 already so warm that i) summer snow falls mostly above the highest reaches of the glaciers, which reduces
383 the interannual variability of summer melt, and ii) conditions close to balanced-budget only occur after
384 snow-rich accumulation seasons.

385 Rapid geometric changes may also lead to a non-linear response of B_a to atmospheric changes, at least for
386 some glaciers. For example, the multiple regression residuals of the Careser Glacier, which were mostly
387 positive in the 1980s, 1990s and 2000s, became predominantly negative after 2008 (Fig. 10). This change
388 may suggest that the rapid modifications occurred in the latest years could have induced a negative
389 feedback, reducing the mass loss rate of the glacier, whose current surface and shape are strongly different
390 from the recent past (inset in Fig. 10). Because the multiple regression model does not use the Oct-May
391 temperature as an explanatory variable, it cannot account for the effects of the warm accumulation season
392 of 2006-07, which led to a very low B_w , early disappearance of winter snow and positive albedo feedback.
393 Therefore, the year 2007 results in highly positive regression residuals.

394

395 **4.3 Future requirements**

396 A common characteristic for all glaciers analysed is their very low mean AAR in the last decade (Table 2).
397 Accumulation areas were almost inexistent in most glaciers, indicating that they will soon disappear, even
398 without additional warming. Some glaciers are displaying morphological changes that indicate their
399 impending extinction, such as rapid disintegration (e.g., Careser Glacier, Fig. 10) and surface lowering in the
400 upper accumulation area (e.g., Fontana Bianca Glacier). The AARs of approximately 0.25 indicate that
401 accumulation areas still exist in the larger and higher-reaching La Mare and Malavalle glaciers. However,
402 given that balanced-budget conditions require AAR close to 0.55, large mass loss and areal reduction are
403 also expected for these two glaciers to reach equilibrium with the climatic conditions of the last ten years.

404 The forthcoming vanishing of the monitored glaciers put the continuation of their mass balance
405 observations at risk. Recently-started monitoring programs in larger and higher-reaching glaciers, such as
406 Malavalle and La Mare, will ensure continued observations in Val Ridanna and the Ortles-Cevedale. In line
407 with the recommendations from the WGMS (Zemp et al., 2009), similar observation programs should start
408 in other large and high-reaching glaciers of the Italian Alps, e.g., in the Gran Paradiso group (to substitute
409 Ciardoney and Grand Etrèt) and in other mountain groups. Both the initiation of observations over new
410 glaciers and the replacement of vanishing glaciers will require an assessment of the spatial
411 representativeness of single glaciers through the comparison of the current mass loss rates over wide
412 geographic areas (Haeberli et al., 2013). This assessments can be obtained using modern techniques such
413 as the multi-temporal differencing of digital elevation models, which enable the comparison of mass loss
414 rates in the last years/decades, by means of the geodetic method, over entire regions or mountain ranges
415 (e.g., Paul and Haeberli, 2008; Abermann et al., 2011; Carturan et al., 2013b; Berthier et al., 2014; Fischer et
416 al., 2015). The geodetic mass balance should also help to control the glacier-wide B_a series measured with
417 the direct glaciological method, and to construct a constant-geometry mass balance record (Elsberg et al.,
418 2001) to be connected to climatic drivers.

419

420 **5 Conclusions**

421 In this work, we have analysed the time series of the glaciers with mass balance observations in the Italian
422 Alps. Based on the results of the analyses, the following conclusions can be drawn:

- 423 ▪ All examined glaciers are experiencing imbalanced conditions, and the longer series show sustained
424 negative trends of B_a .
- 425 ▪ The observed behaviour was mainly caused by increased ablation, led by warmer temperature and
426 related feedbacks. The total precipitation does not show any significant trend, but the fraction of
427 solid precipitation decreased as a consequence of the warmer temperature.
- 428 ▪ The B_a of the analysed glaciers is mainly correlated to B_s , except for two glaciers where windborne
429 snow enhances the importance of B_w . For most glaciers, approximately two thirds of the B_a variance
430 can be explained by multiple linear regression, using the Oct-May precipitation and Jun-Sep
431 temperature as independent variables.
- 432 ▪ The monitored Italian glaciers have comparable mass loss rates to a sample of representative
433 glaciers of the entire European Alps. However, the moving correlation analyses and time series of
434 residuals from multiple linear regressions suggest that the smaller (and thinner) Italian glaciers may
435 be reacting faster to atmospheric changes.
- 436 ▪ Large scale circulation patterns, such as the NAO, have opposite effects in the northern and
437 southern sides of the European Alps. Most of the Italian mass balance series are anti-correlated to
438 the synoptic signal held by the NAO index, through both winter and summer components,
439 sometimes with a strong link. However, in some cases the link is weak or absent and there is not a
440 clear spatial structure.
- 441 ▪ Most monitored glaciers have no more accumulation area and are at risk of extinction, even
442 without additional warming. Therefore, they will soon require a replacement with larger and higher
443 glaciers that retain accumulation areas.

444 ▪ Regional assessments of the mass loss rates using the geodetic method are required to identify
445 possible replacing glaciers, evaluate their spatial representativeness and enable the transitions
446 from replaced to replacing glaciers, as suggested by Haeberli et al. (2013).

447

448 **Author contribution**

449 M. Brunetti processed the meteorological data and prepared the synthetic meteorological series used in
450 this work. Thomas Zanoner compiled the database of the mass balance data and geometric characteristics
451 of the glaciers. L. Carturan and Giulia Zuecco performed the temporal and statistical analyses of the mass
452 balance series. L. Carturan prepared the manuscript with contributions from all co-authors.

453

454 **Acknowledgments**

455 This study was funded by the Italian MIUR Project (PRIN 2010-11): "Response of morphoclimatic system
456 dynamics to global changes and related geomorphological hazards" (local and national coordinators G.
457 Dalla Fontana and C. Baroni). The authors acknowledge the regional environmental agencies of Piemonte,
458 Val d'Aosta, Lombardia, Autonomous Provinces of Trento and Bolzano, which provided the meteorological
459 and topographic data used in this study. Many thanks to Stephan Galos (University of Innsbruck) for sharing
460 information on glaciers in Ötztal and South Tyrol. We would also like to thank all investigators and
461 contributing institutions for the collection and free exchange of the glacier mass balance series. Etienne
462 Bertier and two anonymous referees provided useful suggestions in the review process.

463

464 **References**

465 Abermann, J., Lambrecht, A., Fischer, A., and Kuhn, M.: Quantifying changes and trends in glacier area and
466 volume in the Austrian Ötztal Alps (1969-1997-2006), *The Cryosphere*, 3, 205-215, doi:10.5194/tc-3-205-
467 2009, 2009.

468 Abermann, J., Kuhn, M., and Fischer, A.: Climatic controls of glacier distribution and glacier changes in
469 Austria. *Ann. Glaciol.*, 52(59), 83-90, 2011.

470 Auer, I., Böhm, R., Jurkovic, A., Lipa, W., Orlik, A., Potzmann, R., Schöner, W., Ungersböck, M., Matulla, C.,
471 Briffa, K., Jones, P., Efthymiadis, D., Brunetti, M., Nanni, T., Maugeri, M., Mercalli, L., Mestre, O., Moisselin,
472 J.-M., Begert, M., Müller-Westermeier, G., Kveton, V., Bochnicek, O., Stastny, P., Lapin, M., Szalai, S.,
473 Szentimrey, T., Cegnar, T., Dolinar, M., Gajic-Capka, M., Zaninovic, K., Majstorovic, Z., and Nieplova, E.:
474 HISTALP - Historical Instrumental climatological Surface Time series of the greater ALPine Region, *Int. J.*
475 *Climatol.*, 27, 17-46, doi: 10.1002/joc.1377, 2007.

476 Baroni, C., Bondesan, A., and Mortara, G.: Report of the Glaciological Survey of 2011 - Relazioni della
477 campagna glaciologica 2011, *Geogr. Fis. Din. Quat.*, 35(2), 211-279, doi:10.4461/GFDQ.2012.35.19, 2012.

478 Baroni, C., Bondesan, A., and Mortara, G.: Report of the Glaciological Survey of 2012 - Relazioni della
479 campagna glaciologica 2012, *Geogr. Fis. Din. Quat.*, 36(2), 303-374, doi: 10.4461/GFDQ.2013.36.24, 2013.

480 Baroni, C., Bondesan, A., and Mortara, G.: Report of the Glaciological Survey 2013. Relazioni della
481 Campagna Glaciologica 2013, *Geogr. Fis. Din. Quat.*, 37, 163-227, doi: 10.4461/GFDQ.2014.37.16, 2014.

482 Beniston, M., Keller, F., Koffi, B., and Goyette, S.: Estimates of snow accumulation and volume in the Swiss
483 Alps under changing climatic conditions, *Theor. Appl. Climatol.*, 76, 125–140, doi: 10.1007/s00704-003-
484 0016-5, 2003.

485 Benn, D. I. and Evans, D. J. A. (Eds.): *Glaciers and Glaciation*, Hodder Education, London, UK, 802 pp., 2010.

486 Berthier, E., Vincent, C., Magnússon, E., Gunnlaugsson, Á. Þ., Pitte, P., Le Meur, E., Masiokas, M., Ruiz, L.,
487 Pálsson, F., Belart, J. M. C., and Wagnon, P.: Glacier topography and elevation changes derived from
488 Pléiades sub-meter stereo images, *The Cryosphere*, 8, 2275-2291, doi:10.5194/tc-8-2275-2014, 2014.

489 Braithwaite, R. J., and Olesen, O. B.: Detection of climate signal by inter-stake correlations of annual
490 ablation data Qamanârssûp Sermia, West Greenland, *J. Glaciol.*, 35(120), 253-259, 1989.

491 Brunetti, M., Maugeri, M., Nanni, T., Auer, I., Böhm, R., and Schöner, W.: Precipitation variability and
492 changes in the Greater Alpine region over the 1800–2003 period, *J. Geophys. Res.*, 111, D11107, doi:
493 10.1029/2005/D06674, 2006.

494 Brunetti, M., Lentini, G., Maugeri, M., Nanni, T., Auer, I., Böhm, R., and Schöner, W.: Climate variability and
495 change in the Greater Alpine Region over the last two centuries based on multi-variable analysis, *Int. J.*
496 *Climatol.*, 29(15), 2197-2225, doi: 10.1002/joc.1857, 2009.

497 Brunetti, M., Lentini, G., Maugeri, M., Nanni, T., Simolo, C., and Spinoni, J.: Projecting North Eastern Italy
498 temperature and precipitation secular records onto a high resolution grid, *Phys. Chem. Earth*, 40-41, 9-22,
499 doi: 10.1016/j.pce.2009.12.005, 2012.

500 Brunetti, M., Maugeri, M., Nanni, T., Simolo, C., and Spinoni, J.: High-resolution temperature climatology
501 for Italy: interpolation method intercomparison. *Int. J. Climatol.*, 34, 1278-1296, doi: 10.1002/joc.3764,
502 2014.

503 Cannone, N., Diolaiuti, G., Guglielmin, M., and Smiraglia, C.: Accelerating climate change impacts on alpine
504 glacier forefield ecosystems in the European Alps, *Ecol. Appl.*, 18(3), 637-648, doi: 10.1890/07-1188.1, 2008.

505 Carturan, L., Baroni, C., Becker, M., Bellin, A., Cainelli, O., Carton, A., Casarotto, C., Dalla Fontana, G., Godio,
506 A., Martinelli, T., Salvatore, M. C., and Seppi, R.: Decay of a long-term monitored glacier: Careser Glacier
507 (Ortles-Cevedale, European Alps), *The Cryosphere*, 7, 1819-1838, doi:10.5194/tc-7-1819-2013, 2013a.

508 Carturan, L., Filippi, R., Seppi, R., Gabrielli, P., Notarnicola, C., Bertoldi, L., Paul, F., Rastner, P., Cazorzi, F.,
509 Dinale, R., and Dalla Fontana, G.: Area and volume loss of the glaciers in the Ortles-Cevedale group (Eastern
510 Italian Alps): controls and imbalance of the remaining glaciers, *The Cryosphere*, 7, 1339-1359,
511 doi:10.5194/tc-7-1339-2013, 2013b.

512 Carturan, L., Baldassi, G. A., Bondesan, A., Calligaro, S., Carton, A., Cazorzi, F., Dalla Fontana, G., Francese, R.,
513 Guarnieri, A., Milan, N., Moro, D., and Tarolli, P.: Current behavior and dynamics of the lowermost Italian
514 glacier (Montasio Occidentale, Julian Alps), *Geogr. Ann. A*, 95(1), 79-96, doi: 10.1111/geoa.12002, 2013c.

515 Carturan, L.: Replacing monitored glaciers undergoing extinction: a new measurement series on La Mare
516 Glacier (Ortles-Cevedale, Italy), *J. Glaciol.*, in review, 2016.

- 517 Casartelli, G., Kappenberger, G., and Smiraglia, C.: Accumulo e ablazione sui ghiacciai delle alpi lombarde e
518 svizzere: Risultati di alcuni recenti bilanci di massa, *Rivista Geografica Italiana*, 103(1), 1-30, 1996.
- 519 Catasta, G., and Smiraglia, C.: The mass balance of a cirque glacier in the Italian Alps (Ghiacciaio della
520 Sforzellina, Ortles-Cevedale Group), *J. Glaciol.*, 39(131), 87-90, 1993.
- 521 CGI (Comitato Glaciologico Italiano): Reports of the glaciological surveys, *Bollettino del Comitato*
522 *Glaciologico Italiano*, Series I and II, 1–25, 1914–1977.
- 523 CGI (Comitato Glaciologico Italiano): Reports of the glaciological surveys, *Geogr. Fis. Din. Quat.*, 1–35, 1978–
524 2011.
- 525 Cogley, J. G.: Geodetic and direct mass-balance measurements: comparison and joint analysis. *Ann. Glaciol.*,
526 50(50), 96-100, 2009.
- 527 Cogley, J. G., and Adams, W. P.: Mass balance of glaciers other than the ice sheets, *J. Glaciol.*, 44(147), 315-
528 325, 1998.
- 529 Cogley, J. G., Hock, R., Rasmussen, L. A., Arendt, A. A., Bauder, A., Braithwaite, R. J., Jansson, P., Kaser, G.,
530 Moller, M., Nicholson, L., and Zemp, M.: Glossary of Glacier Mass Balance and Related Terms, IHP-VII
531 Technical Documents in Hydrology No. 86, IACS Contribution No. 2, UNESCO-IHP, Paris, 2011.
- 532 Colucci, R. R., and Guglielmin, M.: Precipitation–temperature changes and evolution of a small glacier in the
533 southeastern European Alps during the last 90 years, *Int. J. Climatol.*, 35(10), 2783–2797,
534 doi: 10.1002/joc.4172, 2015.
- 535 Debeer, C. M., and Sharp, M. J.: Topographic influences on recent changes of very small glaciers in the
536 Monashee Mountains, British Columbia, Canada, *J. Glaciol.*, 55(192), 691–700, doi:
537 10.3189/002214309789470851, 2009.
- 538 Durand, Y., Laternser, M., Giraud, G., Etchevers, P., Lesaffre, B., and Mérindol, L.: Reanalysis of 44 years of
539 climate in the French Alps (1958–2002): methodology, model validation, climatology, and trends for air
540 temperature and precipitation, *J. Appl. Meteorol. Climatol.*, 48(3), 429–449, 2009a.
- 541 Durand, Y., Giraud, G., Laternser, M., Etchevers, P., Mérindol, L., and Lesaffre, B.: Reanalysis of 47 years of
542 climate in the French Alps (1958–2005): climatology and trends for snow cover, *J. Appl. Meteorol. Climatol.*,
543 48(12), 2487–2512, 2009b.
- 544 Dyurgerov, M., Meier, M. F., and Bahr, D. B.: A new index of glacier area change: a tool for glacier
545 monitoring, *J. Glaciol.*, 55(192), 710-716, 2009.
- 546 Eckert, N., Baya, H., Thibert, E., and Vincent, C.: Extracting the temporal signal from a winter and summer
547 mass-balance series: application to a six-decade record at Glacier de Sarennes, French Alps, *J. Glaciol.*,
548 57(201), 134-150, 2011.
- 549 Elsberg, D. H., Harrison, W. D., Echelmeyer, K. A., and Krimmel, R. M.: Quantifying the effect of climate and
550 surface change on glacier mass balance, *J. Glaciol.*, 47, 649–658, 2001.
- 551 Fischer, M., Huss, M., and Hoelzle, M.: Surface elevation and mass changes of all Swiss glaciers 1980–2010,
552 *The Cryosphere*, 9, 525-540, doi:10.5194/tc-9-525-2015, 2015.

- 553 Furbish, D. J., and Andrews, J. T.: The use of hypsometry to indicate long-term stability and response of
554 valley glaciers to changes in mass transfer, *J. Glaciol.*, 30, 199–211, 1984.
- 555 Galos, S. P., Klug, C., Prinz, R., Rieg, L., Dinale, R., Sailer, R., and Kaser, G.: Recent glacier changes and
556 related contribution potential to river discharge in the Vinschgau / Val Venosta, Italian Alps, *Geogr. Fis. Din.*
557 *Quat.*, 38, 143-154, doi: 10.4461/GFDQ.2015.38.13, 2015.
- 558 Haeberli, W., Huggel, C., Paul, F., and Zemp, M.: Glacial responses to climate change, in: *Treatise on*
559 *Geomorphology*, Academic Press, 13, San Diego, California, 152-175, 2013.
- 560 Hoelzle, M., Haeberli, W., Dischl, M., and Peschke, W.: Secular glacier mass balances derived from
561 cumulative glacier length changes, *Global Planet. Change*, 36, 295–306, doi: 10.1016/S0921-
562 8181(02)00223-0, 2003.
- 563 Huss, M., Dhulst, L., and Bauder, A.: New long-term mass balance series for the Swiss Alps, *J. Glaciol.*,
564 61(227), 551-562, doi: 10.3189/2015JoG15j015, 2015.
- 565 Kaser, G., Fountain, A., and Jansson, P.: A manual for monitoring the mass balance of mountain glaciers,
566 IHP-VI Technical Documents in Hydrology No. 59, UNESCO-IHP, Paris, 2003.
- 567 Killick, R., Eckley, I. A.: Changepoint: An R package for changepoint analysis, *J. Stat. Softw.*, 58(3), 1-19. DOI:
568 10.18637/jss.v058.i03, 2014.
- 569 Kuhn, M.: The mass balance of very small glaciers, *Zeitschrift für Gletscherkunde und Glazialgeologie*, 31(1–
570 2), 171–179, 1995.
- 571 Lliboutry, L.: Multivariate statistical analysis of glacier annual balances, *J. Glaciol.*, 13, 371-392, 1974.
- 572 Marzeion, B. and Nesje, A.: Spatial patterns of North Atlantic Oscillation influence on mass balance
573 variability of European glaciers, *The Cryosphere*, 6, 661-673, doi:10.5194/tc-6-661-2012, 2012.
- 574 Mernild, S. H., Lipscomb, W. H., Bahr, D. B., Radić, V., and Zemp, M.: Global glacier changes: a revised
575 assessment of committed mass losses and sampling uncertainties, *The Cryosphere*, 7, 1565-1577,
576 doi:10.5194/tc-7-1565-2013, 2013.
- 577 Mitchell, T. D., and Jones, P. D.: An improved method of constructing a database of monthly climate
578 observations and associated high-resolution grids, *Int. J. Climatol.* 25, 693–712, doi: 10.1002/joc.1181, 2005.
- 579 New, M., Hulme, M., and Jones, P. D.: Representing twentieth century space-time variability. Part 2:
580 development of 1901–96 monthly grids of surface climate, *J. Climate*, 13, 2217–2238, 2000.
- 581 Oerlemans, J., and Reichert, B. K.: Relating glacier mass balance to meteorological data by using a seasonal
582 sensitivity characteristic, *J. Glaciol.*, 46(152), 1–6, doi: 10.3189/172756500781833269, 2000.
- 583 Østrem, G., and Brugman, M.: Mass balance measurement techniques. A manual for field and office work,
584 National Hydrology Research Institute (NHRI), Science Report, (4), Saskatoon, Canada, 224 pp., 1991.
- 585 Paul, F., and Haeberli, W.: Spatial variability of glacier elevation changes in the Swiss Alps obtained from
586 two digital elevation models, *Geophys. Res. Lett.*, 35, L21502, doi:10.1029/2008GL034718, 2008.

587 Pelto, M. S.: Glacier annual balance measurement, forecasting and climate correlations, North Cascades,
588 Washington 1984–2006, *The Cryosphere*, 2, 13-21, doi:10.5194/tc-2-13-2008, 2008

589 Quadrelli, R., Lazzeri, M., Cacciamani, C., and Tibaldi, S.: Observed winter Alpine precipitation variability and
590 links with large-scale circulation patterns, *Clim. Res.*, 17(3), 275-284, doi:10.3354/cr017275, 2001.

591 Reichert, B. K., Bengtsson, L., and Oerlemans, J.: Midlatitude forcing mechanisms for glacier 25 mass
592 balance investigated using general circulation models, *J. Climate*, 14, 3767–3784, 2001.

593 Salvatore, M. C., Zanoner, T., Baroni, C., Carton, A., Banchieri, F. A., Viani, C., Giardino, M., and Perotti, L.:
594 The state of Italian glaciers: a snapshot of the 2006-2007 hydrological period, *Geogr. Fis. Dinam. Quat.*, 38,
595 175-198, 2015.

596 Schmidli, J., Schmutz, C., Frei, C., Wanner, H., and Schär, C.: Mesoscale precipitation variability in the region
597 of the European Alps during the 20th century, *Int. J. Climatol.*, 22(9), 1049-1074, doi: 10.1002/joc.769, 2002.

598 Schöner, W., Auer, I., and Böhm, R.: Climate variability and glacier reaction in the Austrian eastern Alps,
599 *Ann. Glaciol.*, 31(1), 31-38, 2000.

600 Schwarb, M.: The alpine precipitation climate, Ph.D. thesis, ETH Zürich, Switzerland, 131 pp., 2000.

601 Scotti, R., Brardinoni, F., and Crosta, G. B.: Post-LIA glacier changes along a latitudinal transect in the
602 Central Italian Alps, *The Cryosphere*, 8, 2235-2252, doi:10.5194/tc-8-2235-2014, 2014.

603 Six, D., Reynaud, L., and Letréguilly, A.: Alpine and Scandinavian glaciers mass balances, their relations with
604 the North Atlantic Oscillation, *Comptes Rendus de l'Académie des Sciences, Series IIA, Earth Planet. Sc.*, 333,
605 693–698, 2001.

606 Thibert, E., Eckert, N., and Vincent, C.: Climatic drivers of seasonal glacier mass balances: an analysis of 6
607 decades at Glacier de Sarennes (French Alps), *The Cryosphere*, 7(1), 47-66, 2013.

608 Vincent, C., Kappenberger, G., Valla, F., Bauder, A., Funk, M., and Le Meur, E.: Ice ablation as evidence of
609 climate change in the Alps over the 20th century, *J. Geophys. Res.*, 109(D10), D10104, doi:
610 10.1029/2003JD003857, 2004.

611 WGMS: Global glacier changes: facts and figures, edited by: Zemp, M., Roer, I., Kaab, A., Hoelzle, M., Paul,
612 F., and Haerberli, W., UNEP, World Glacier Monitoring Service, Zürich, Switzerland, 2008.

613 WGMS: Fluctuations of Glaciers 2005-2010, Volume X, edited by: Zemp, M., Frey, H., Gärtner-Roer, I.,
614 Nussbaumer, S. U., Hoelzle, M., Paul, F., and W. Haeberli: ICSU(WDS)/IUGG(IACS)/UNEP/UNESCO/WMO,
615 World Glacier Monitoring Service, Zurich, Switzerland, 336 pp., publication based on database version:
616 doi:10.5904/wgms-fog-2012-11, 2012.

617 WGMS: Glacier Mass Balance Bulletin No. 12 (2010-2011), edited by: Zemp, M., Nussbaumer, S. U., Naegeli,
618 K., Gärtner-Roer, I., Paul, F., Hoelzle, M., and Haeberli, W.: ICSU(WDS)/IUGG(IACS)/UNEP/UNESCO/WMO,
619 World Glacier Monitoring Service, Zurich, Switzerland, 106 pp., publication based on database version: doi:
620 10.5904/wgms-fog-2013-11, 2013.

621 WGMS: Fluctuations of Glaciers Database. World Glacier Monitoring Service, Zurich, Switzerland.
622 DOI:10.5904/wgms-fog-2015-11, 2015. Online access: <http://dx.doi.org/10.5904/wgms-fog-2015-11>

623 Zemp, M., Frauenfelder, R., Haeberli, W., and Hoelzle, M.: Worldwide glacier mass balance measurements:
624 general trends and first results of the extraordinary year 2003 in Central Europe, *Data of Glaciological*
625 *Studies [Materialy glyatsiologicheskikh issledovani]*, 99, Moscow, Russia, 3–12, 2005.

626 Zemp, M., Paul, F., Hoelzle, M., and Haeberli, W.: Glacier fluctuations in the European Alps 1850-2000: an
627 overview and spatio-temporal analysis of available data, in *The darkening peaks: Glacial retreat in scientific*
628 *and social context*, edited by: Orlove, B., Wiegandt, E., and Luckman, B. H., University of California Press,
629 Berkeley, 152-167, 2008.

630 Zemp, M., Hoelzle, M., and Haeberli, W.: Six decades of glacier mass-balance observations: a review of the
631 worldwide monitoring network, *Ann. Glaciol.*, 50(50), 101-111, doi: 10.3189/172756409787769591, 2009.

632 Zemp, M., Thibert, E., Huss, M., Stumm, D., Rolstad Denby, C., Nuth, C., Nussbaumer, S. U., Moholdt, G.,
633 Mercer, A., Mayer, C., Joerg, P. C., Jansson, P., Hynek, B., Fischer, A., Escher-Vetter, H., Elvehøy, H., and
634 Andreassen, L. M.: Reanalysing glacier mass balance measurement series. *The Cryosphere*, 7, 1227-1245,
635 doi:10.5194/tc-7-1227-2013, 2013.

636

637

638

639

Tables

640 Table 1 – Physical characteristics of the Italian glaciers with the mass balance series analysed in this study
 641 (year 2006, NextData - DATAGRALP project: [http://www.nextdatapoint.it/?q=en/content/special-project-](http://www.nextdatapoint.it/?q=en/content/special-project-datagrulp)
 642 [datagrulp](http://www.nextdatapoint.it/?q=en/content/special-project-datagrulp), last access: 27 September 2015; Salvatore et al., 2015).

| Glacier | Geographic area | Area (km ²) | Minimum elevation (m a.s.l.) | Maximum elevation (m a.s.l.) | Median elevation (m a.s.l.) | Prevailing aspect | Average slope (°) | First survey year |
|---------------------------|-----------------|-------------------------|------------------------------|------------------------------|-----------------------------|-------------------|-------------------|-------------------|
| Grand Etrèt | Gran Paradiso | 0.47 | 2667 | 3190 | 2894 | N | 23 | 2002 |
| Ciardoney | Gran Paradiso | 0.59 | 2855 | 3170 | 3039 | E-NE | 18 | 1992 |
| Fontana Bianca | Ortles-Cevedale | 0.48 | 2889 | 3342 | 3166 | E | 23 | 1984 |
| Sforzellina | Ortles-Cevedale | 0.29 | 2790 | 3046 | 2868 | NW | 16 | 1987 |
| Lunga | Ortles-Cevedale | 1.86 | 2678 | 3378 | 3128 | NE | 19 | 2004 |
| Careser | Ortles-Cevedale | 2.39 | 2868 | 3279 | 3069 | S | 11 | 1967 |
| La Mare (southern branch) | Ortles-Cevedale | 2.16 | 2652 | 3518 | 3215 | NE | 21 | 2003 |
| Pendente | Val Ridanna | 0.95 | 2621 | 3064 | 2781 | S | 15 | 1996 |
| Malavalle | Val Ridanna | 6.92 | 2512 | 3441 | 2971 | SE | 14 | 2002 |

643

644

645

646 Table 2 – Mean values (and STD in brackets) of B_w , B_s , B_a and AAR for nine Italian glaciers in the period from
 647 2004 to 2013 (Car = Careser, FB = Fontana Bianca, Pen = Pendente, Cia = Ciardoney, Sfo = Sforzellina, GE =
 648 Grand Etrèt, Lun = Lunga, Mar = La Mare, Mal = Malavalle). Values expressed in mm w.e. except AAR that is
 649 in percent.

| | Car | Mar | FB | Sfo | Lun | Pen | Mal | Cia | GE |
|--------------------|----------------|----------------|----------------|----------------|----------------|----------------|----------------|----------------|----------------|
| B_w (9 years) | 927 (330) | 989 (301) | 1085 (338) | \ | 991 (222) | 1537 (425) | 1194 (256) | 1052 (421) | 1472 (578) |
| B_s (9 years) | -2740 (368) | -1758 (303) | -2183 (457) | \ | -2151 (368) | -2857 (525) | -2087 (386) | -2510 (378) | -2396 (321) |
| B_a (10 years) | -1788 (590) | -763 (395) | -1088 (642) | -1399 (505) | -1195 (466) | -1231 (692) | -825 (484) | -1419 (646) | -946 (648) |
| AAR (10 years) | 1 (3) | 25 (14) | 11 (22) | \ | 12 (16) | 4 (8) | 23 (17) | 3 (5) | \ |

650

651

652

653 Table 3 – Correlation matrix of B_a for nine Italian glaciers. * and ** indicate Spearman correlation significant
654 at the 0.05 and 0.01 level, respectively.

| | Car | FB | Pen | Cia | Sfo | GE | Lun | Mar | Mal |
|-----|--------|--------|--------|--------|--------|--------|-------|--------|------|
| Car | 1.00 | | | | | | | | |
| FB | 0.82** | 1.00 | | | | | | | |
| Pen | 0.85** | 0.76** | 1.00 | | | | | | |
| Cia | 0.87** | 0.86** | 0.55* | 1.00 | | | | | |
| Sfo | 0.82** | 0.75** | 0.65** | 0.81** | 1.00 | | | | |
| GE | 0.74** | 0.77** | 0.66* | 0.62* | 0.69* | 1.00 | | | |
| Lun | 0.70* | 0.73* | 0.60 | 0.48 | 0.49 | 0.77** | 1.00 | | |
| Mar | 0.90** | 0.96** | 0.70* | 0.90** | 0.82** | 0.80** | 0.71* | 1.00 | |
| Mal | 0.87** | 0.84** | 0.97** | 0.61* | 0.65* | 0.68* | 0.61 | 0.80** | 1.00 |

655

656

657

658 Table 4 – Correlation coefficients of B_a vs. B_w and B_s . * and ** indicate Spearman correlation significant at
659 the 0.05 and 0.01 level, respectively.

| | No of years | B_w | B_s |
|-----|-------------|--------|--------|
| Car | 40 | 0.46** | 0.94** |
| FB | 22 | 0.24 | 0.84** |
| Pen | 12 | 0.84** | 0.67* |
| Cia | 22 | 0.51* | 0.76** |
| GE | 12 | 0.84** | 0.66* |
| Lun | 10 | 0.64* | 0.69* |
| Mar | 10 | 0.66* | 0.64* |
| Mal | 9 | 0.48 | 0.85** |

660

661

662

663 Table 5 – Correlation coefficients of B_w , B_s and B_a vs. seasonal and annual NAO. Five-year triangular moving
 664 averages have been applied to the time series before correlation analyses. *, ** and *** indicate Spearman
 665 correlation significant at the 0.10, 0.05 and 0.01 level, respectively.

666

| Nation | Glacier | Winter balance | | | Summer balance | | | Annual balance | | |
|--------|------------|----------------|-------------|------------|----------------|-------------|------------|----------------|-------------|------------|
| | | DJF NAO | Oct-May NAO | Annual NAO | DJF NAO | Oct-May NAO | Annual NAO | DJF NAO | Oct-May NAO | Annual NAO |
| I | Car | -0.51** | -0.34 | -0.16 | -0.23 | -0.05 | 0.34 | -0.30* | -0.13 | 0.23 |
| I | FB | -0.11 | 0.18 | 0.00 | 0.22 | 0.10 | 0.25 | 0.07 | 0.35 | 0.41* |
| I | Pen | -0.70 | -0.90* | -0.70 | -1.00** | -0.90* | -1.00** | 0.12 | 0.15 | 0.23 |
| I | Cia | 0.17 | 0.34 | 0.19 | -0.03 | 0.10 | 0.27 | 0.13 | 0.27 | 0.36 |
| I | GE | -0.81*** | -0.74** | -0.79** | -0.88*** | -0.76** | -0.91*** | -0.86*** | -0.76** | -0.83*** |
| I | Lun | -0.94** | -0.94** | -0.94** | -0.94** | -0.77 | -0.94** | -0.89** | -0.83* | -0.89** |
| I | Mar | -1.00*** | -0.89** | -1.00*** | 0.14 | 0.03 | 0.14 | -0.79** | -0.82** | -0.89*** |
| I | Mal | -0.90* | -0.70 | -0.90* | -0.50 | -0.80 | -0.50 | -0.81*** | -0.74** | -0.45 |
| I | Sfo | | | | | | | 0.59*** | 0.59*** | 0.61*** |
| F | St. Sorlin | | | | | | | -0.44*** | -0.38*** | -0.04 |
| F | Sarennes | 0.36*** | 0.43*** | 0.49*** | -0.53*** | -0.50*** | -0.19 | -0.41*** | -0.37*** | -0.05 |
| CH | Silvretta | 0.28* | 0.13 | -0.05 | -0.57*** | -0.45*** | -0.18 | -0.38*** | -0.28** | 0.02 |
| CH | Gries | -0.39*** | -0.22 | -0.18 | -0.58*** | -0.53*** | -0.25* | -0.49*** | -0.39*** | -0.03 |
| A | Sonnblick | | | | | | | -0.48*** | -0.45*** | -0.07 |
| A | Vernagt | 0.27* | 0.51*** | 0.49*** | -0.42*** | -0.38** | -0.09 | -0.36** | -0.26* | 0.07 |
| A | Kesselwand | | | | | | | -0.42*** | -0.38*** | -0.07 |
| A | Hintereis | | | | | | | -0.55*** | -0.44*** | -0.10 |

667

668

669

670 Table 6 - Spearman correlation coefficients and multiple regression results of B_a vs. seasonal mean
 671 temperature and precipitation. *, ** and *** indicate 0.05, 0.01 and 0.001 significance levels.

| Air temperature – Correlation coefficients | | | | | | | | | |
|---|--------------------|--------------------|--------------------|-------------------|------------------|---------------|--------------|----------------------------|-----------------------|
| | Car | FB | Sfo | Cia | Pen | GE | Mal | Mar | Lun |
| No of years | 47 | 27 | 27 | 22 | 18 | 12 | 12 | 11 | 10 |
| Jun-Sep | -0.77*** | -0.49** | -0.52** | -0.64** | -0.40 | 0.01 | -0.24 | -0.16 | 0.49 |
| Oct-May | -0.37** | -0.42* | -0.10 | -0.18 | -0.49* | -0.18 | -0.57 | -0.28 | -0.33 |
| Year | -0.68*** | -0.49** | -0.30 | -0.49* | -0.69** | -0.31 | -0.71** | -0.27 | -0.14 |
| Precipitation – Correlation coefficients | | | | | | | | | |
| | Car | FB | Sfo | Cia | Pen | GE | Mal | Mar | Lun |
| No of years | 47 | 27 | 27 | 22 | 18 | 12 | 12 | 11 | 10 |
| Jun-Sep | -0.15 | -0.02 | 0.09 | 0.20 | 0.00 | 0.02 | -0.04 | 0.26 | -0.05 |
| Oct-May | 0.28 | 0.40* | 0.32 | 0.47* | 0.37 | 0.57 | 0.43 | 0.67* | 0.71* |
| Year | 0.11 | 0.36 | 0.39* | 0.53* | 0.34 | 0.64* | 0.34 | 0.83** | 0.53 |
| Multiple linear regression - Coefficients | | | | | | | | | |
| | Car | FB | Sfo | Cia | Pen | GE | Mal | Mar | Lun |
| No of years | 47 | 27 | 27 | 22 | 18 | 12 | 12 | 11 | 10 |
| Jun-Sep temperature | -776.453 (***) | -663.487 (***) | -575.225 (***) | -796.739 (***) | -496.521 (**) | -63.899 | -355.106 | -668.941 (**) | 115.265 |
| Oct-May precipitation | 2.186 (***) | 3.342 (***) | 2.915 (***) | 3.315 (***) | 2.380 (*) | 2.897 (**) | 3.051 (*) | 4.122 (**) | 2.666 (*) |
| Intercept | -3265.013 (***) | -3311.632 (***) | -3176.797 (***) | 1753.826 | 1011.719 | -2707.559 | 19.212 | - 3380.90 5 (***) | - 2619.872 (**) |
| % of explained variance | 75.6 | 68.7 | 72.1 | 73.7 | 51.5 | 56.8 | 56.0 | 78.4 | 64.5 |

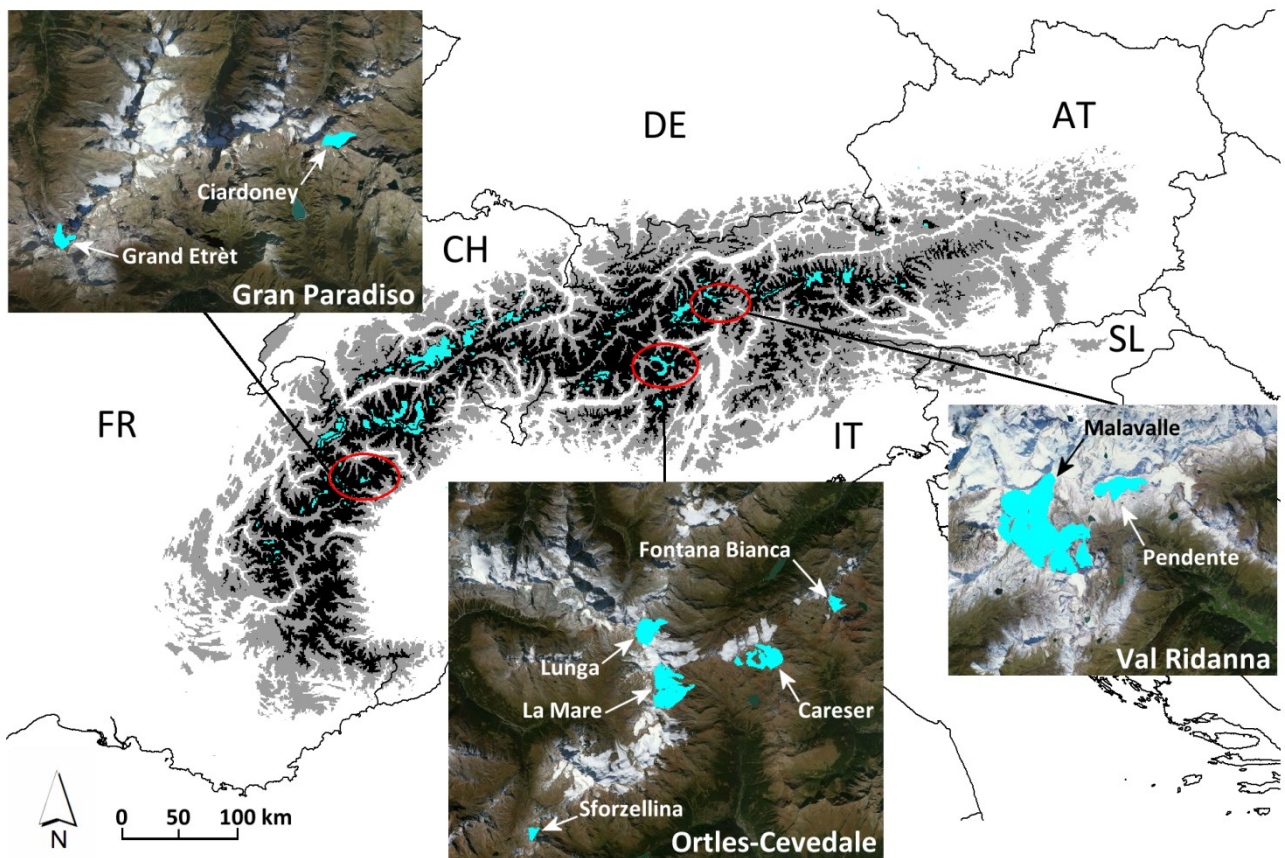
672

673

674

Figures

675

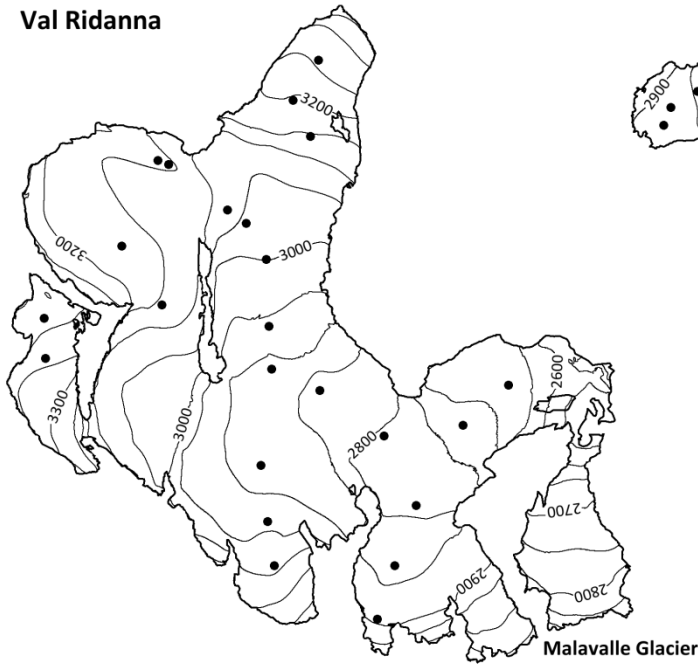


676

677 Figure 1. Geographic setting of the glaciers with mass balance measurements analysed in this work
678 (Microsoft® BingTM Maps).

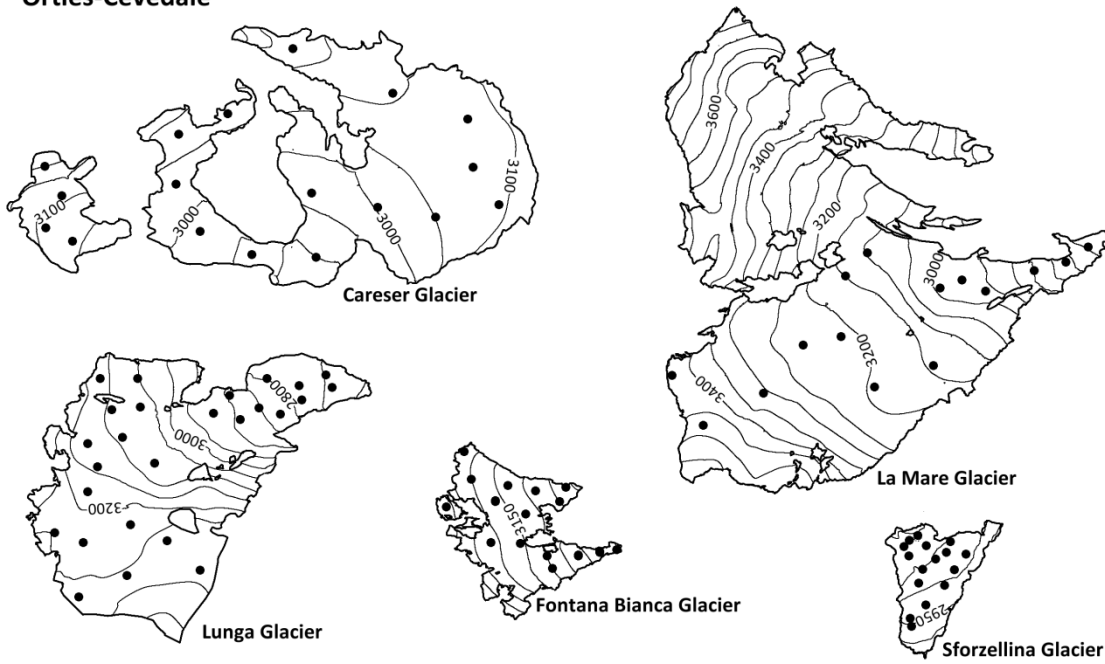
679

Val Ridanna

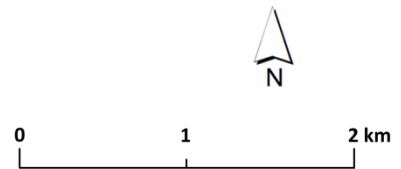
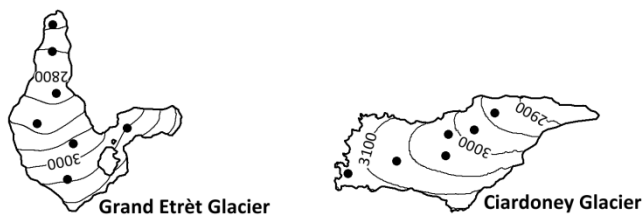


- Mass balance measurement points
- Contours (height interval = 50 m)

Ortles-Cevedale



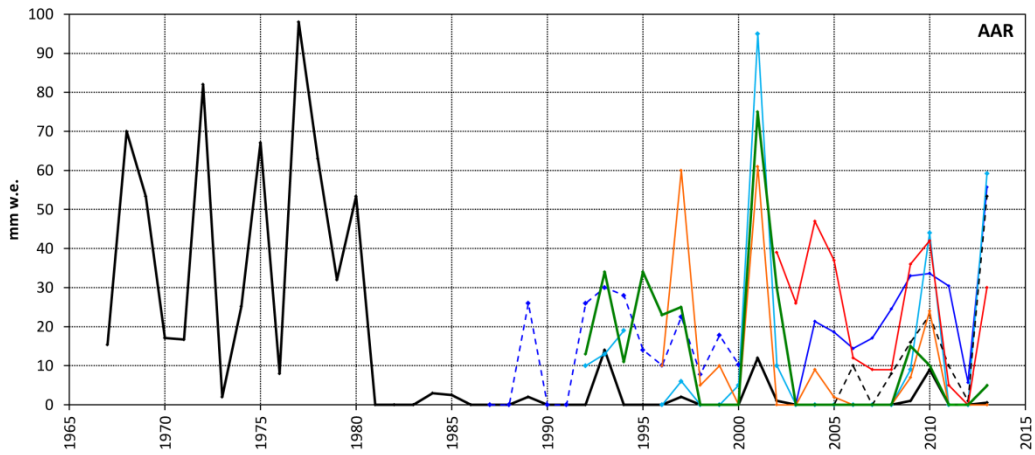
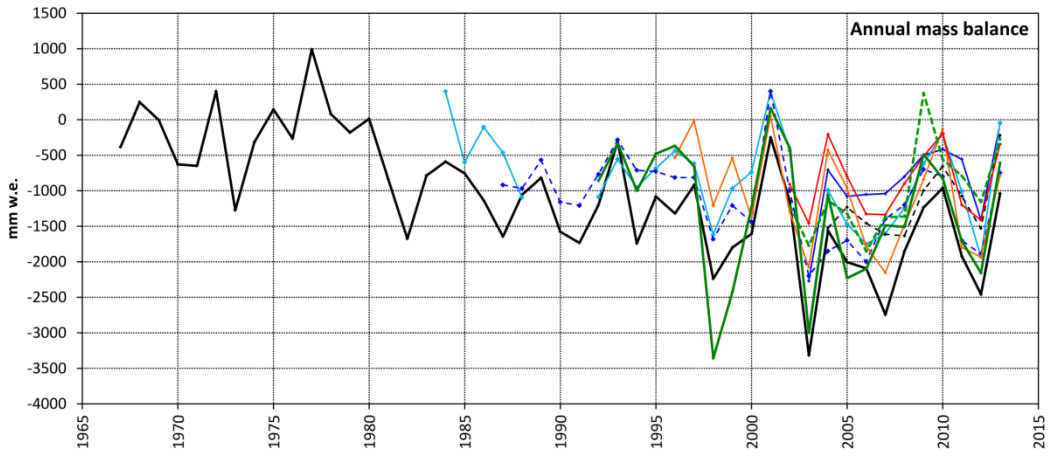
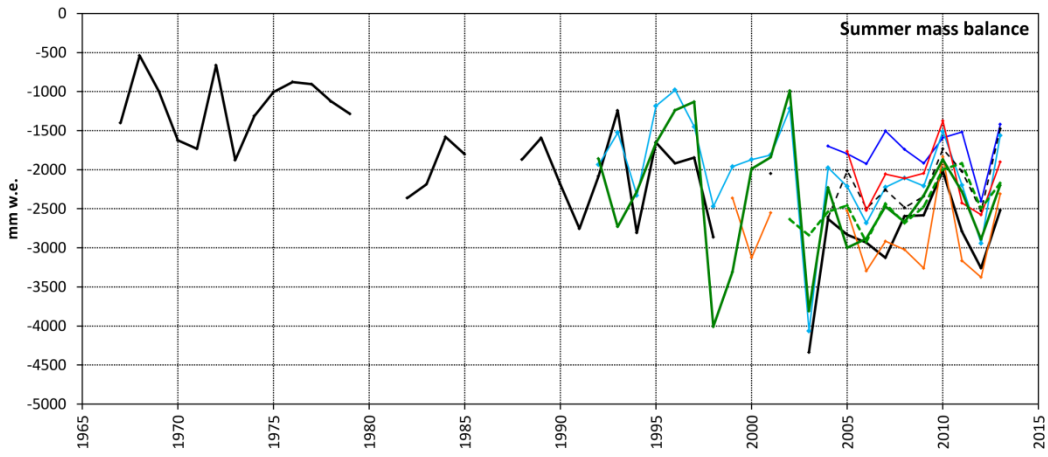
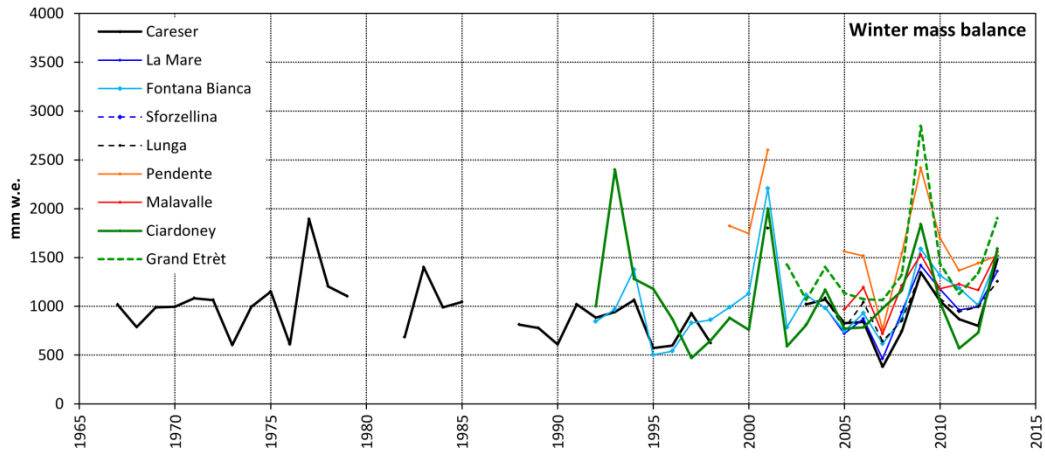
Gran Paradiso



680

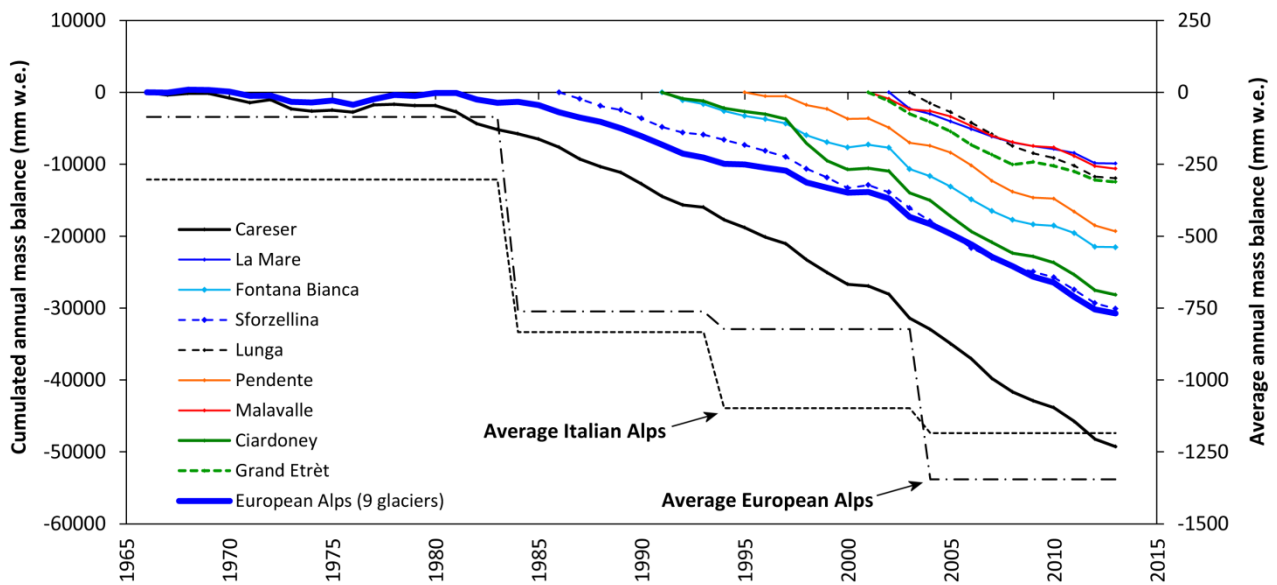
681

Figure 2. Surface topography and measurement network of the nine glaciers analysed in this study.



683 Figure 3. Time series of B_w , B_s , B_a and AAR for the nine Italian glaciers analysed.

684

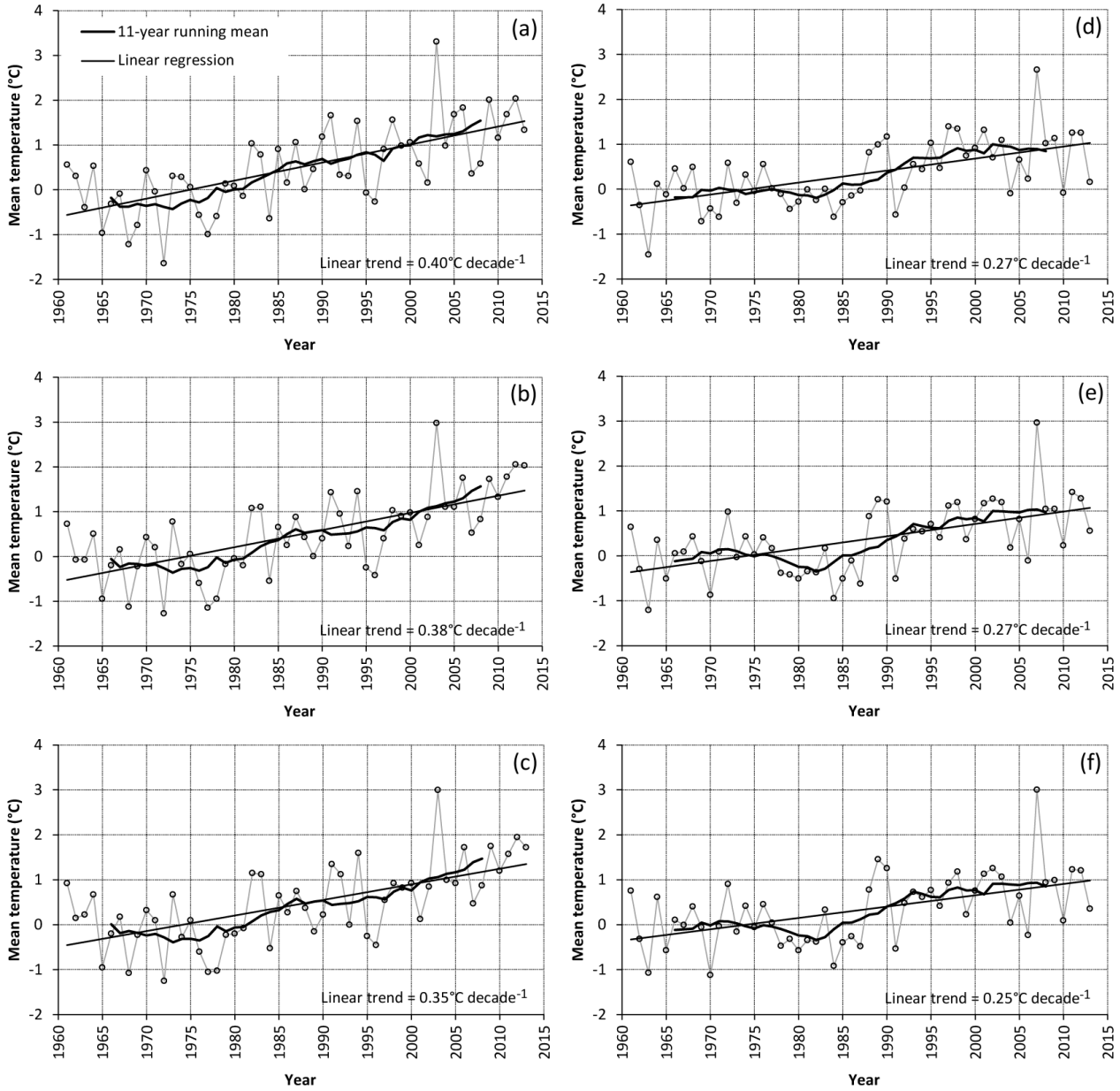


685

686 Figure 4. Cumulative mass balance for the nine Italian glaciers and for a set of nine other glaciers
687 representative of the European Alps. Dotted and dashed lines indicate the average B_a for the two groups of
688 glaciers in the periods from 1967 to 1983, 1984 to 1993, 1994 to 2003 and 2004 to 2013.

689

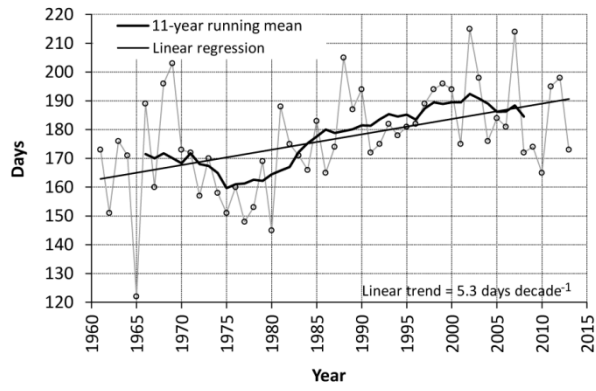
690



691

692 Figure 5. Left column: mean ablation season (Jun-Sep) air temperature anomalies in (a) Gran Paradiso, (b)
 693 Ortles-Cevedale, and (c) Val Ridanna. Right column: mean accumulation season (Oct-May) air temperature
 694 anomalies in (d) Gran Paradiso, (e) Ortles-Cevedale, and (f) Val Ridanna. Reference period: 1961-1990. All
 695 linear trends are significant at the 0.001 level.

696



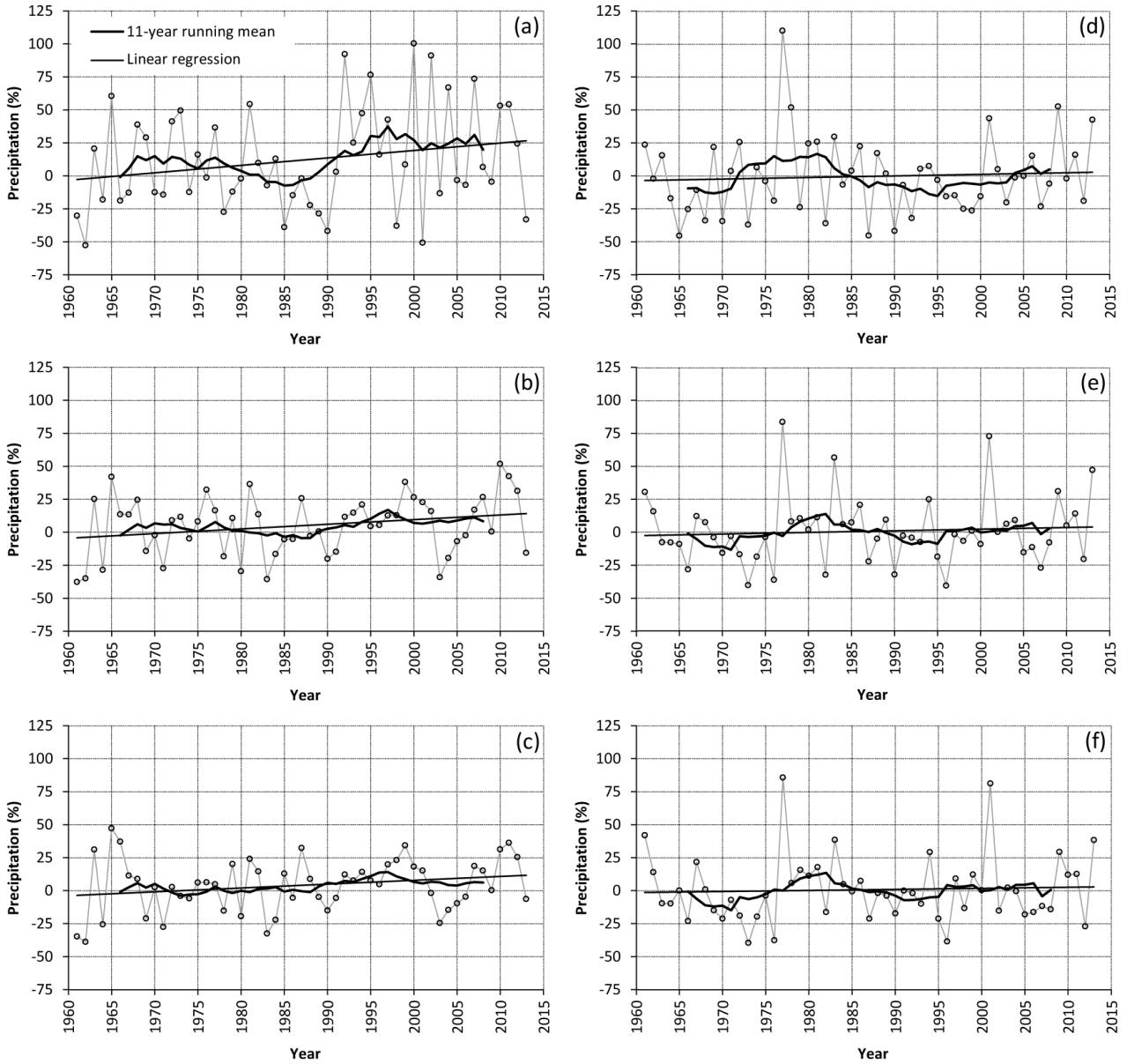
697

698 Figure 6. Days per year with maximum air temperature exceeding 0°C at 3000 m a.s.l., calculated from the
 699 series of the Careser diga weather station (2600 m a.s.l., Ortles-Cevedale Group).

700

701

702



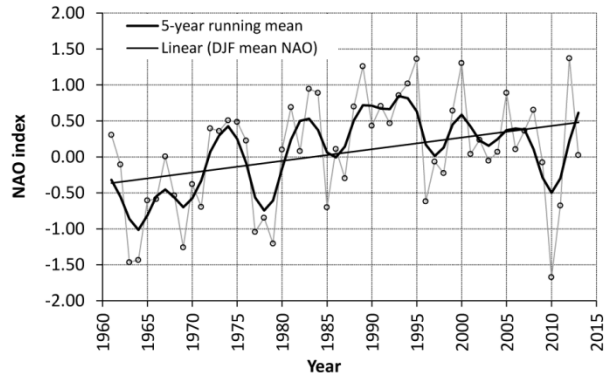
703

704 Figure 7. Left column: ablation season (Jun-Sep) total precipitation anomalies in (a) Gran Paradiso, (b)
 705 Ortles-Cevedale, and (c) Val Ridanna. Right column: accumulation season (Oct-May) total precipitation
 706 anomalies in (d) Gran Paradiso, (e) Ortles-Cevedale, and (f) Val Ridanna. Reference period: 1961-1990. None
 707 of the linear trends is significant at the 0.05 level.

708

709

710



711

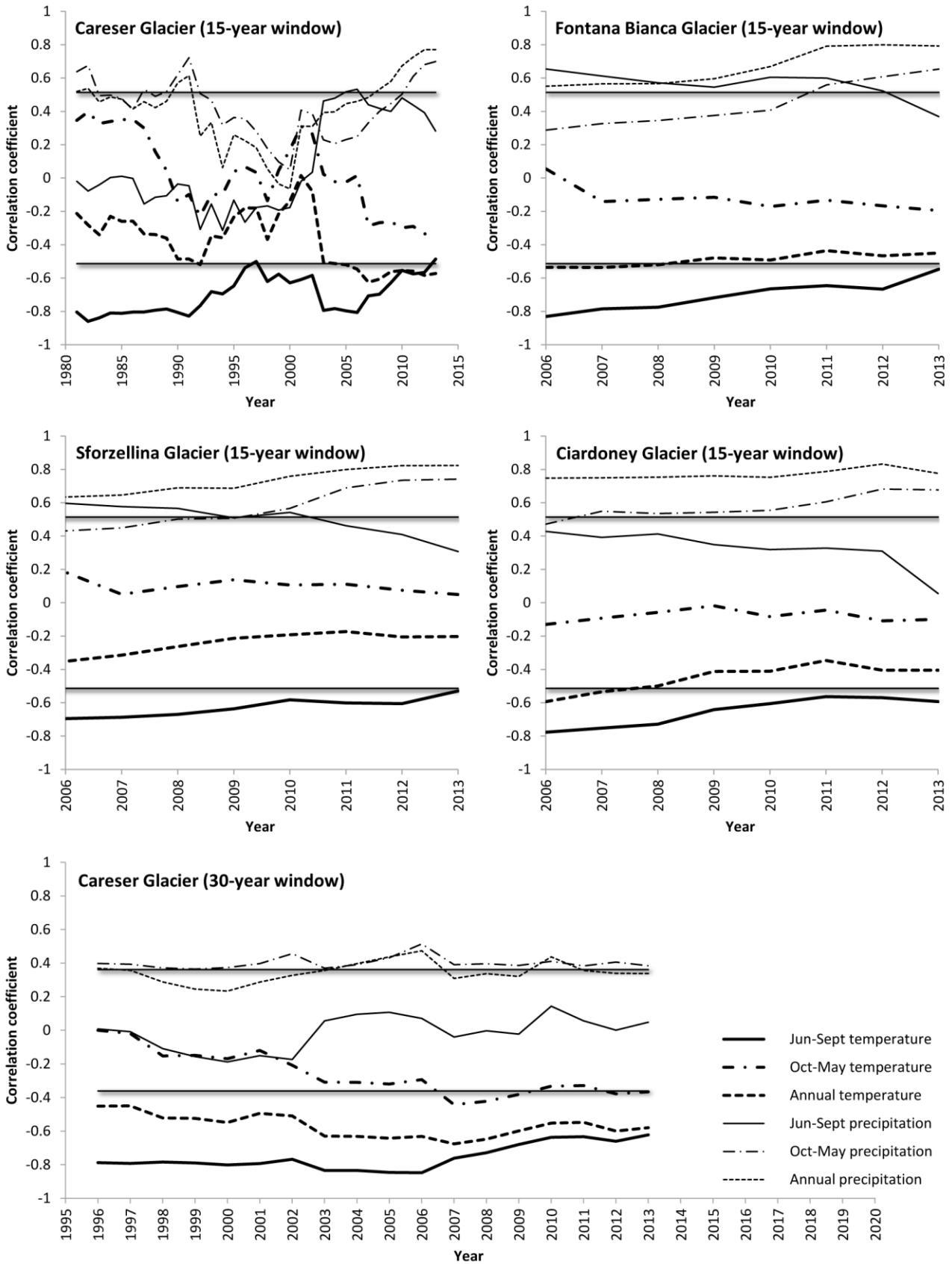
712

713

714

715

Figure 8. Winter NAO index from 1961 to 2013
 (<http://www.cpc.ncep.noaa.gov/products/precip/CWlink/pna/new.nao.shtml>, last access: 11 February 2016).

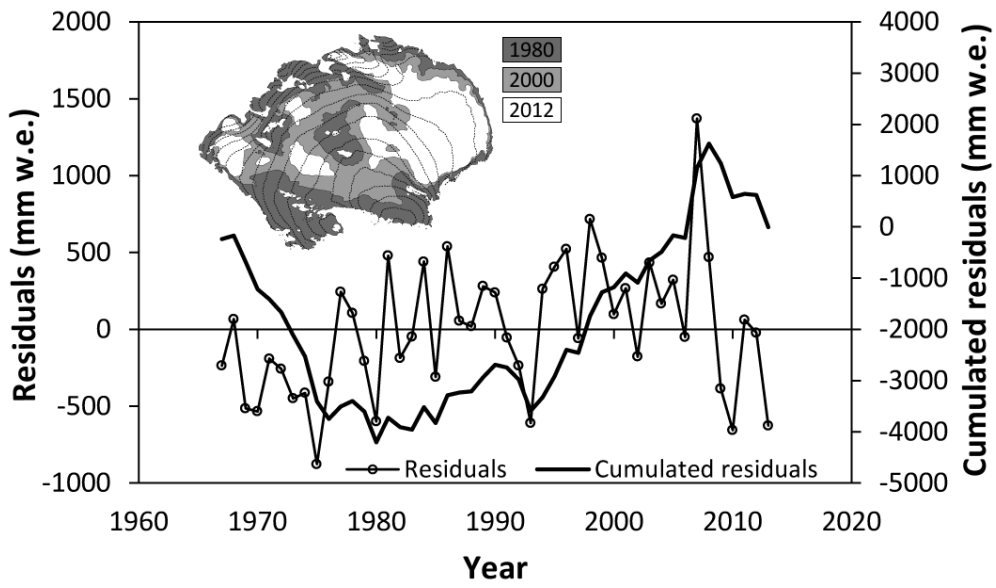


716

717 Figure 9. Bootstrapped moving correlation coefficient between annual mass balance and seasonal values of
 718 air temperature and precipitation. Shaded straight lines indicate significance at 95% level.

719

720



721

722 Figure 10. Plot of residuals of the multiple linear regression of B_a vs. Oct-May precipitation and Jun-Sep
723 temperature on the Careser Glacier. Multiple regression coefficients are reported in Table 6. The inset
724 shows the extent of the glacier in three different years.

725

726

727

728

729

730

731

732

733

734

735

736

737